The Role of Protons In and Around Biradicals for Cross-Effect Dynamic Nuclear Polarization

Satyaki Chatterjee,[a] Amrit Venkatesh,[b] Snorri Th. Sigurdsson,*[a] Frédéric Mentink-Vigier*[b]

In magic angle spinning dynamic nuclear polarization, biradicals such as bis-nitroxides are used to hyperpolarize protons under microwave irradiation through the cross-effect mechanism. This mechanism relies on electron-electron spin interactions (dipolar coupling and exchange interaction) and electron to nuclear spin interactions (hyperfine coupling) to hyperpolarize the protons surrounding the biradical. This hyperpolarization is then transferred to the bulk sample via nuclear spin diffusion. However, the involvement of the protons in the biradical in the cross-effect DNP process has been under debate. In this work, we address this question by exploring the hyperpolarization pathways in and around bis-nitroxides. We demonstrate that for biradicals with strong electron-electron interactions, as in the case of the AsymPols, the protons on the biradical may not be necessary to quickly generate hyperpolarization. Instead, such biradicals can efficiently, and directly, polarize the surrounding protons of the solvent. The findings should impact the design of the next generation of biradicals.

Introduction

Solid-state Nuclear Magnetic Resonance (NMR) is one of the most potent way to access atomic-scale information on solids.[1] However, the inherent low sensitivity of solid-state NMR limits its application to investigate low concentrations of NMR active species. This limited sensitivity primarily arises from the low polarization level of the nuclear spins at thermal equilibrium. On the other hand, electron spins have larger spin polarization, due to their higher gyromagnetic ratio ($\gamma_e/\gamma_{1H} \sim 658$). Using the coupling between electron and nearby nuclear spins and using microwave (μw) irradiation at an appropriate frequency, one can increase the nuclear spin polarization through a process called Dynamic Nuclear Polarization (DNP).[2]

In the past decades, DNP has been combined with Magic Angle Spinning (MAS) at high magnetic fields using high-power μw sources, which has enabled the acquisition of MAS NMR spectra with high resolution and sensitivity.[3–10] DNP has revolutionized the field of solid-state NMR and enabled numerous applications both for biological and material samples,[11–23] in particular at natural isotopic abundance.[24–27]

As of today, MAS-DNP is best carried out using biradicals as polarizing agents,[28,29] that generate high nuclear spin hyperpolarization via a mechanism called cross-effect (CE).[30–33] Biradicals are paramagnetic molecules, with two unpaired electrons spins, that are dissolved in glass-forming matrices such as glycerol/water mixtures and typically used to polarize the protons present in these matrices. The hyperpolarization can be subsequently transferred to the nuclear spins of interest via cross polarization.[34]

The cross-effect DNP mechanism relies on optimal relative *g*-tensor orientations in the biradical,[32,35–38] strong interelectron spin couplings,[39–44] and sufficiently long electron spin relaxation times. Nuclear hyperpolarization has been improved by preparing bulky molecules,[45–49] and by designing pathways for polarization transfer.[50] Importantly, the cross-effect DNP mechanism relies on the existence of a coupling between the radical centres through space (dipolar coupling, $D_{a,b}$) and through overlap of orbitals (exchange interaction, $J_{a,b}$) – cumulatively these interactions are referred to as e-e couplings, hereafter. In addition, the Electron Paramagnetic Resonance (EPR) spectral width ($\Delta\omega$) of the biradicals must be greater than the Larmor frequency of the protons.

The detailed analysis of this mechanism DNP under MAS has been the subject of several previously reports.[30–33,36,51,52] Briefly, the μw irradiation generates a polarization difference between the two electron spins in the biradical that is transferred to nearby protons. These events occur periodically due to the spinning of the sample and the large breadth of the EPR spectrum, and have been dubbed 'rotor events'.[32] The transfer of the electron spins polarization difference to the proton spins occurs during the cross-effect rotor events. The rate of electron to nucleus polarization transfer involves the e-e couplings, the pseudo-secular hyperfine couplings between electron and proton spins ($A^{\pm}_{a,n}$ and $A^{\pm}_{b,n}$), and the inverse of the Larmor frequency of the nucleus (ω_n).[31,32,53]

Using the Landau-Zener approximation under MAS, the initial rate of the polarization transfer between the biradical and the nuclear spin can be expressed as follows (see Supporting Information for details):

$$R_{\mathrm{CE}} \propto \frac{1}{\Delta\omega_a + \Delta\omega_b} \left| \frac{\left(D_{a,b} + 2J_{a,b}\right)\left(A^{\pm}_{a,n} - A^{\pm}_{b,n}\right)}{\omega_n} \right|^2 . \qquad (1)$$

As such, the cross-effect can polarize protons that are close to the electron spins, and the resulting nuclear hyperpolarization is then transferred to protons further way via nuclear spin diffusion.[54] Thus, protons that are close are essential for receiving the hyperpolarization and transmitting the hyperpolarization away from the biradical.

Under standard DNP experimental conditions, proton homonuclear spin diffusion is rapid.[55,56] Indeed, protons far away from the biradical (hereafter referred to as bulk protons) have very similar Larmor frequencies and strong dipolar couplings resulting in an efficient homonuclear spin diffusion. However, the

[a] University of Iceland, Department of Chemistry, Science Institute, Dunhaga 3, 107 Reykjavik (Iceland)
[b] National High Magnetic Field Laboratory, Florida State University, 1800 E. Paul Dirac Dr, Tallahassee, FL, 32310.
Email: snorrisi@hi.is, fmentink@magnet.fsu.edu

spin diffusion between the protons in the vicinity of the biradical and the ones further away is hindered by the presence of the hyperfine couplings that change their effective Larmor frequency, resulting in a slow transmission of polarization to the bulk protons. The region where these nearby protons with sizeable hyperfine couplings belong to is often referred as the spin diffusion barrier, and its role in the DNP process has been the subject of a long-standing debate.[50,57–60]

In recent years, the role of these nearby protons has been under scrutiny. The advent of numerical models that are able to account for a large number of nuclear spins has highlighted the importance of protons near the biradical.[53,61–63] It has been shown that these nearby protons can periodically exchange their polarization when their Larmor frequency is equal via nuclear dipolar rotor events[32,53,63,64] and thus are essential to the DNP process under MAS.

Lately, the protons on the biradicals have been the centre of an extensive study, for example in the case of the bTbK biradical family[35] that possess modest $D_{a,b} \sim 30$ MHz.[61,65] In this comprehensive work, the authors selectively deuterated TEKPol[66] and showed that removing the protons on the molecule lead to slower hyperpolarization process. These observations highlight the importance of strong electron-nuclear hyperfine couplings in the cross-effect rate, in agreement with equation (1).

On the other hand, equation (1) also shows that the initial polarization transfer rate can be modulated by changing the e-e couplings. This rationale was the basis of the design of the AsymPol family of biradicals (Figure 2).[40,41] The AsymPols were designed using a conjugated amide linker that enables a close proximity between the two moieties leading to large couplings with $D_{a,b} = 56$ MHz and $J_{a,b} \sim 95$ and 120 MHz (for each of the two conformers).[41] These strong e-e couplings result in increased cross-effect rates and therefore, AsymPol biradicals can generate hyperpolarization very quickly.[40,41]

In this article we explore how such strong e-e couplings affects the MAS-DNP process around the biradicals. We focus on the role of the protons on the biradicals and demonstrate both theoretically and experimentally that protons on the AsymPols are not required for hyperpolarization, and that the nuclear hyperpolarization can be generated very quickly outside of the molecule. We begin by demonstrating the ability of the numerical methods to predict the behaviour of nuclear spin hyperpolarization build-up times in MAS-DNP experiments for several cases. We then study the role of the protons on AMUPol[67] and on a AsymPol derivative from a theoretical point of view by selective deuteration of the molecules. The predictions were then verified experimentally on AsymPol-COOK which is a new derivative of the AsymPol family. We finally discuss how the hyperpolarization is transferred in both cases and its experimental consequences.

Results

The effect of the initial polarization transfer can be observed by the characteristic time it takes to generates the hyperpolarization called build-up time, T_B. It has been demonstrated that the measured build-up time reflects the combined effects of the initial CE polarization rate and the spin diffusion rate (inside and outside of the so-called spin diffusion barrier).[57] It is important to first demonstrate that our model is robust enough for predicting the build-up time under different conditions, to explain how the hyperpolarization is transferred to the bulk and to identify which protons are involved in the process. In the next section we illustrate the ability of the code to do so under various conditions.

Benchmarking the MAS-DNP model

The MAS-DNP simulations were performed using the previously introduced multi-nuclei model.[41,63] This model simulates the MAS-DNP process with biradicals placed at the center of a box made of the matrix in which it is dissolved. This model is suitable to represent how the polarization is transferred from the biradical to the bulk nuclei and thus predict T_B.

Table 1: Evolution of the polarization build-up time, T_B, as a function of the main magnetic field strength for 5 or 10 mM AMUPol in d_8-glycerol/D_2O/H_2O (6/3/1 volume ratio), [^{1}H] = 11 M

	T_B (s)			
B_0, MAS freq.	exp (10 mM)	sim (10 mM)	exp (5 mM)	sim (5 mM)
9.4 T, 8 kHz	3.5[67]	3.6	-	7.3
9.4 T, 40 kHz	3.8[68]	4.1	7.1[68]	7.7
14.1 T, 8 kHz	4.8[63,67]	4.5	-	8.7
18.8 T, 8 kHz	5[69]	5	15[68]	10.2
18.8 T, 40 kHz[69]	6.6	6.1	18[68]	11.3

The calculations use structures obtained from Molecular Dynamics (MD) simulations as input and describe the MAS-DNP process and the spin diffusion around the biradical, under certain approximations.[41,63] It makes extensive use of the Landau-Zener approximation applied in the Liouville space[53] to ensure a linear scaling of the problem with the number of spins. In addition, the model takes as input the biradical geometry, e-e coupling, and electron to proton interactions. All these parameters can be reasonably obtained from density functional theory (DFT).[41,61,63] We note that both isotropic (Fermi contact) and anisotropic (dipolar) hyperfine couplings are calculated using DFT simulations and are essential to accurately predict the build-up times, as has also been noted previously.[41,50,63] Since this model was developed to simulate simple cases of AMUPol or AsymPol-POK at 10 mM concentration for moderate MAS frequency, and proton concentration [^{1}H] = 11 M,[41,63] we verified its ability to simulate cases beyond its initial focus. It should be noted that the model is able to predict the T_B of AsymPol-POK.[41]

First, we tested the model on the well characterized AMUPol biradical ((Figure 2). AMUPol is a water soluble bis-nitroxide introduced by Sauvee et *al.*[67] It possesses relatively strong e-e

couplings with $D_{a,b} = 35$ MHz and $J_{a,b} = -15$ MHz.[61,70] Under MAS, $D_{a,b} + 2J_{a,b}$ ranges from -100 to 20 MHz which enables relatively short build-up times. As such AMUPol is an excellent polarizing agent.

Table 1 reports T_B as function of the main magnetic field intensity for AMUPol when [^{1}H] = 11 M and different MAS frequencies (8 or 40 KHz). The corresponding simulations shows a good agreement with the experiments: the magnetic field and MAS frequency trends are clearly reproduced for both biradical concentrations (Table 1). Note that the enhancements were also calculated (SI), however the box model is not able to accurately calculate the enhancements, as previously noted.[61,71]

To further test the robustness of the model, T_B was simulated for different proton concentrations and compared with the results recently published by Prisco et al (Figure 1).[57] The excellent agreement between experiments and simulations demonstrates the validity of this multi-nuclei model used in the simulations.

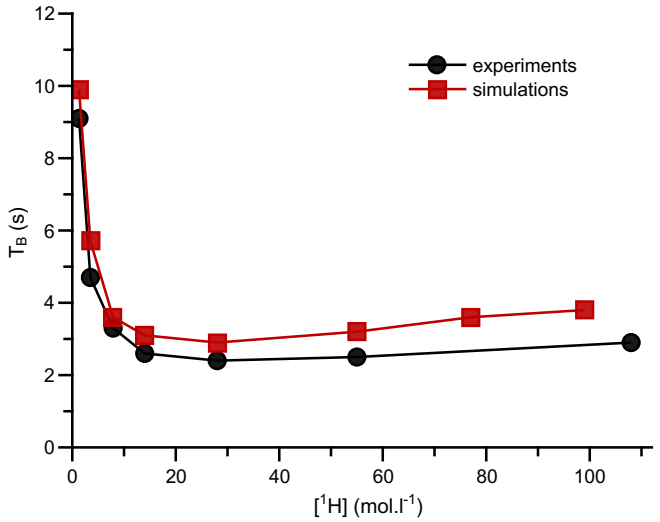

Figure 1: Plot showing T_B as a function of [^{1}H] for 12 mM AMUPol dissolved in mixtures of glycerol/H_2O (6/4 volume ratio) and d_8-glycerol/D_2O (6/4 volume ratio). Black circles, experimental data extracted from ref [57], red squares, simulations.

MAS-DNP simulations with AMUPol and AsymPol-OH

We subsequently explored the impact of degree of deuteration of the radicals (Figure 2) on the DNP build-up times at two different magnetic fields, 9.4 T and 14.1 T (Figure 3). To simplify the MD simulations, a neutral AsymPol, AsymPol-OH was used for predictions as its geometry is very similar to AsymPol-POK.[41]

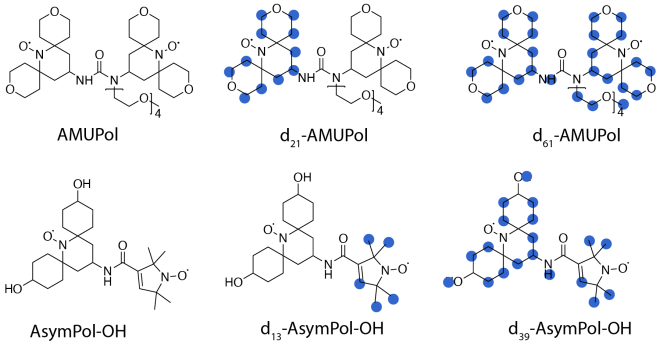

Figure 2: Biradical structures tested for MAS-DNP, deuterated sites are indicated in blue.

First the non-deuterated biradicals were tested *in silico* (Figure 3); AsymPol-OH yield much faster build-up times than AMUPol. At both 9.4 T and 14.1 T, AsymPol-OH was predicted to have build-up times three-fold shorter than AMUPol (1 s vs 3.6 s and 1.8 vs 4.5 s, respectively, Figure 3).

The simulations were then carried out for the biradicals where only one moiety was deuterated. In that case the build-up time of AMUPol increases to 4.1 s and 5.8 s at 9.4 T and 14.1 T, respectively (Figure 3). On the other hand, the build-up times of AsymPol-OH are unaffected by deuteration.

When the biradicals are fully deuterated, similar trends are observed: the build-up time of AMUPol becomes significantly longer (7.5 and 11 s at 9.4 T and 14.1 T, respectively), while the build-up time of AsymPol-OH only increases negligibly and remains very close to 1 and 1.8 s at 9.4 and 14.1 T, respectively.

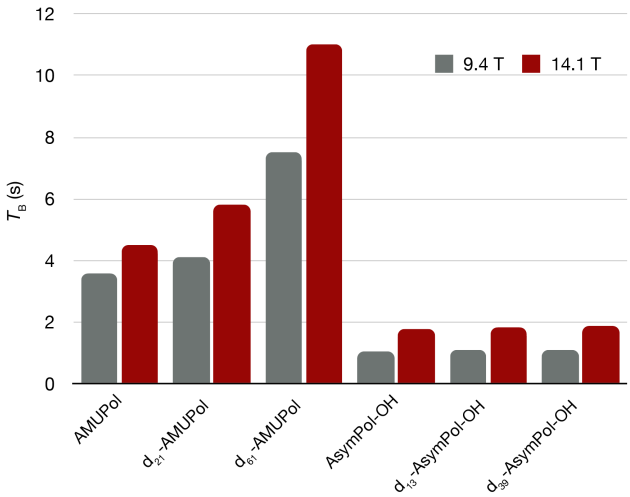

Figure 3: Calculated build-up times for 10 mM AMUPol or 10 mM AsymPol-OH dissolved in d_8-Glycerol/D_2O/H_2O. Three different deuteration levels of the biradicals have been simulated: no deuteration, one radical moiety deuterated, and fully deuterated.

These simulations show differing trends: for AMUPol, the protons on the biradicals are essentials for generating quick nuclear hyperpolarization, while there is no apparent role for these protons in the propagation of hyperpolarization for AsymPol-OH.

MAS DNP experiments with AsymPol-COOK

To verify the predictions, we carried out the synthesis of AsymPol-COOK (Scheme 1, SI) as well as d_{12}-AsymPol-COOK, and tested them experimentally. AsymPol-COOK is a new water-soluble derivative of AsymPol that is easier to synthesize than AsymPol-POK. DFT simulations predict that AsymPol-COOK possesses a very similar structure as to AsymPol-OH (see SI). The MAS-DNP experiments used a 10 mM solution of AsymPol-COOK and d_{12}-AsymPol-COOK in a glass forming matrix made of d_8-glycerol/D_2O/H_2O (6/3/1 volume ratio). The build-up time and enhancement $\epsilon_{\mathrm{on/off}}$ of the two biradicals was measured at 8 kHz and 14.1 T (Table 2). The build-up times are identical for both biradicals, and matches the predictions discussed above. The enhancement for the partially deuterated biradical is higher than for the fully deuterated one. This is in line with previous work that observed that deuterating the methyl groups in alpha of the nitroxides group yields larger enhancements[47,72,73] unlike deuteration in the TEKPol case.[50] Removal of the protons on the fast relaxing methyl groups has been shown to increase electron spin relaxation times, which likely affects the microwave saturation factor and observed enhancements.[47,72,73] These effects are not completely understood and will be the subject of future work.

Table 2 Experimental results of 10 mM of AsymPol-COOK and d_{31}-AsymPol-COOK in d_8-glycerol/D_2O/H_2O (6/3/1 volume ratio).

Biradical	$\epsilon_{\mathrm{on/off}}$	T_B (s)
AsymPol-COOK	70±2	2±0.1
d_{12}-AsymPol-COOK	90±2	2±0.1

Discussion

The generation of hyperpolarization via cross-effect MAS-DNP involves generating an electron spin polarization difference that is transferred to the surrounding nuclei. This process involves the hyperfine couplings and the couplings between the two electron spins in biradicals. Strictly speaking, the efficiency of the polarization transfer depends on the efficiency of the cross-effect rotor events (obtained via the Landau-Zener approximation) and the number of such events per rotor period. These two factors depend on the crystallite orientation but also depend on the relative orientations of the *g*-tensors.[31,32,36] Since the evolution of the proton polarization is slow compared to the MAS rate,[31,53,62,63] we will ignore the discontinuities induced by the rotor events.

The polarization transfer from the radicals to the bulk nuclei can take two different pathways:

1. polarization of the protons on the molecule followed by spin diffusion to the bulk protons,
2. direct polarization of solvent protons followed by spin diffusion to the bulk protons.

These two pathways can coexist, but their relative contribution may depend on the rate of polarization transfer from the biradicals to each proton (i.e. the cross-effect efficiency), and on the rate of the spin diffusion between protons that are strongly coupled to the electron in the region of the spin diffusion barrier (which depends on the density of protons[50]). The two pathways do not possess the same weight when comparing AMUPol and the AsymPols.

The polarization of the protons in and around the biradical can be approximately described as a set of equation connecting the two pools of protons: those that are on the biradical, and those that are in the solvent:

$$\begin{aligned}\frac{dP_{\mathrm{birad}}}{dt} &= -R_{\mathrm{CE}}^{\mathrm{birad}}(P_{\mathrm{birad}} - \Delta P_e) - R_{1,n}^{\mathrm{birad}}(P_{\mathrm{birad}} - P_B) \\ &\quad - R_{\mathrm{SD}}(\mathrm{P}_{\mathrm{birad}} - \mathrm{P}_{\mathrm{solv}}) \\ \frac{dP_{\mathrm{solv}}}{dt} &= -R_{\mathrm{CE}}^{\mathrm{solv}}(P_{\mathrm{solv}} - \Delta P_e) - R_{1,n}^{\mathrm{solv}}(P_{\mathrm{solv}} - P_B) \\ &\quad - R_{\mathrm{SD}}(\mathrm{P}_{\mathrm{solv}} - \mathrm{P}_{\mathrm{birad}}),\end{aligned} \tag{2}$$

where $R_{\mathrm{CE}}^{\mathrm{birad}}$ and $R_{\mathrm{CE}}^{\mathrm{solv}}$ is the average R_{CE} for the protons on the biradicals and in the solvent, respectively, $R_{1,n}^{\mathrm{birad}}$ and $R_{1,n}^{\mathrm{solv}}$ are the nuclear relaxation rate for the protons on the biradicals and in the solvent, respectively, R_{SD} is the spin diffusion or exchange rate between the two pools of protons, P_B is the thermal equilibrium polarization, P_{birad} and P_{solv} are polarization levels of the protons on the biradical molecule and solvent matrix, respectively, and ΔP_e is the absolute value of the polarization difference between the electron spins at steady state.[32,36]

If we assume that differences in the proton distribution around both biradicals are negligible, which results in similar magnitude of hyperfine couplings, then R_{SD}, and $A^{\pm}$ are identical. Furthermore, we assume that the EPR linewidths are also similar for both biradicals ($\Delta\omega_{\mathrm{Asym}} \approx \Delta\omega_{\mathrm{AMU}}$), this implies that the ratio

$$\frac{\nu_{\mathrm{CE}}^{\mathrm{birad}}(\mathrm{AsymPol})}{\nu_{\mathrm{CE}}^{\mathrm{birad}}(\mathrm{AMUPol})} = \frac{\nu_{\mathrm{CE}}^{\mathrm{solv}}(\mathrm{AsymPol})}{\nu_{\mathrm{CE}}^{\mathrm{solv}}(\mathrm{AMUPol})} = \frac{|D_{\mathrm{Asym}}+2J_{\mathrm{Asym}}|^2}{|D_{\mathrm{AMU}}+2J_{\mathrm{AMU}}|^2}, \tag{3}$$

mainly depends on ratio of the strength of the e-e couplings of both biradicals. For AMUPol $|D_{\mathrm{AMU}} + 2J_{\mathrm{AMU}}|$ spans the range of 20-100 MHz, while in the case of AsymPols $|D_{\mathrm{Asym}} + 2J_{\mathrm{Asym}}|$ spans a range of 120-300 MHz. Therefore, the AsymPols can hyperpolarize protons faster by a factor ~ 9-16 on average than AMUPol via a larger R_{CE}. One should note that this ratio is in line with the ratio of the inverse of the build-up times $T_B^{\mathrm{AMU}}/T_B^{\mathrm{Asym}}$ at 9.4 T and 14.1 T.

A consequence of this much stronger R_{CE}, AsymPol can achieve the same polarization rate as AMUPol on protons that are $\approx 9^{1/3}$ to $16^{1/3} \approx 2$ to 2.5 times further. Therefore, AsymPol can more easily hyperpolarize protons in the solvent and does not require the protons on the biradical as predicted by simulations. Since the polarization build-up time of AsymPol is unchanged, $T_B \approx 1.8$ s, this means that the transfer rate R_{SD} between the protons of biradical and those of the solvent indicates is smaller than $R_{\mathrm{CE}}^{\mathrm{solv}}(\mathrm{AsymPol})$. Therefore, the equations become decoupled:

$$\frac{dP_{\mathrm{Asym}}}{dt} = -R_{\mathrm{CE}}^{\mathrm{Asym}}\left(P_{\mathrm{Asym}} - \Delta P_e^{\mathrm{Asym}}\right) - R_{1,n}^{\mathrm{Asym}}\left(P_{\mathrm{Asym}} - P_B\right)$$
$$\frac{dP_{\mathrm{solv}}}{dt} = -R_{\mathrm{CE}}^{\mathrm{solv}}\left(P_{\mathrm{solv}} - \Delta P_e^{\mathrm{Asym}}\right) - R_{1,n}^{\mathrm{solv}}\left(P_{\mathrm{solv}} - P_B\right) \quad (4)$$

In contrast, the large change for T_B in AMUPol vs d_{21}-AMUPol, from 4.5 to 5.8 s, means that $R_{\mathrm{CE}}^{\mathrm{solv}}(\mathrm{AMUPol}) < R_{\mathrm{SD}}$. For AMUPol the equation then becomes:

$$\frac{dP_{\mathrm{AMU}}}{dt} = -R_{\mathrm{CE}}^{\mathrm{AMU}}\left(P_{\mathrm{AMU}} - \Delta P_e^{\mathrm{AMU}}\right) - R_{1,n}^{\mathrm{AMU}}(P_{\mathrm{AMU}} - P_B) - R_{\mathrm{SD}}(\mathrm{P_{AMU}} - P_{\mathrm{solv}})$$
$$\frac{dP_{\mathrm{solv}}}{dt} = -r_{1,n}^{\mathrm{solv}}(P_{\mathrm{solv}} - P_B) - R_{\mathrm{SD}}(P_{\mathrm{solv}} - \mathrm{P_{AMU}}) \quad (5)$$

All in all, the preferred polarization pathways for AMUPol and AsymPol at 14.1 T are shown schematically in Figure 4.

As R_{CE} diminishes with field due to the combined effect of $\Delta\omega_a + \Delta\omega_b$ and ω_n^2 in equation (1) the build-up times tends to be longer at high fields.[68] Under very high field conditions, the protons on the biradicals may once again be important for the AsymPols.

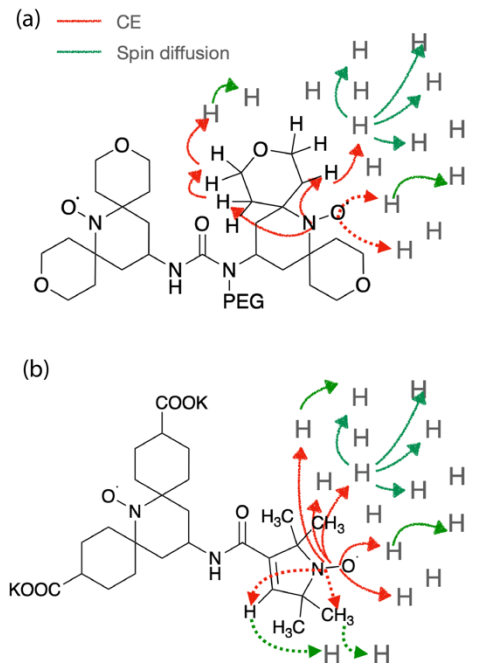

Figure 4: Hyperpolarization pathways for (a) AMUPol and (b) AsymPol-COOK. Red arrows indicate direct polarization transfer via CE, and green arrows indicate proton homonuclear spin diffusion. Full line corresponds to the preferred pathway while dotted lines corresponds to the less favorable one.

We note that in the previous work on the series of deuterated TEKPols,[50] the cross-effect rate is likely limited by relatively low e-e couplings in comparison to the AsymPols. Consequently, the dominant pathway is the hyperpolarization of the closest spins on the biradical molecule. Analogous arguments are also valid for the observations made by Oschkinat and co-workers in the case of TOTAPOL.[73]

Finally, an increase in R_{CE} is desirable but increasing the e-e coupling may not be the only solution. Indeed a large e-e coupling can favor electron-electron cross-relaxation that prevents the generation of large ΔP_e [32] and if larger than $|\omega_n|$ the CE rotor events disappear.[42,44] It is possible that the presence of electron-electron cross-relaxation limits the performance of the AsymPols and other biradicals with large e-e couplings.

Instead an increase in R_{CE} can equivalently be achieved by using biradicals with correct relative orientations (which increases the number of CE rotor events),[36] or by using hetero-biradicals,[42,74,75] i.e. molecules made of two different radical types with different EPR linewidth. The latter impacts $\Delta\omega_a + \Delta\omega_b$ in equation (1).

Conclusions

In this work we have studied the hyperpolarization pathways around two commonly used families of biradicals for MAS-DNP experiments, AMUPol and the AsymPols. After demonstrating that the MAS-DNP simulations can reproduce the experimental build-up times of AMUPol results under numerous conditions, we predicted the effect of biradical deuteration using AMUPol and AsymPol-OH as models. The simulations revealed that T_B for AsymPols do not change under any of the deuteration levels tested. This contrasts with previous reports, notably on the bTbK family[35,50] and indicates a different pathway for the hyperpolarization around the AsymPol. This was confirmed experimentally on AsymPol-COOK, a new water-soluble derivative of AsymPol.

These results show that protons near the radical centers of biradicals with moderate e-e coupling, play a significant role in the hyperpolarization pathways. Another highlight of this work is that the so-called diffusion barrier is rather permissible in the case of MAS-DNP: in this region the hyperpolarization transfer is slowed down, but not quenched as the term “barrier” might imply.

Taken together, our results not only reveal the intricacies of the hyperpolarization mechanism, but also demonstrate that when the e-e couplings are large, protons on the biradical are not necessary. Next generation of biradicals should thus focus on increasing the e-e interaction but also improve the relative g-tensor orientation or build on the potential of hetero-biradicals. This will favor an efficient polarization transfer even in difficult media, i.e. fully protonated media,[41,57] but also cases where the targeted nuclear spin is low concentration or is not present on the biradical, e.g. ^{19}F.

Acknowledgements

The National High Magnetic Field laboratory (NHMFL) is funded by the National Science Foundation Division of Materials Research (DMR-1644779 and DMR-2128556) and the State of Florida. A portion of this work was supported by the NIH P41 GM122698 and RM1-GM148766. This project has received partial support from the European Union's Horizon 2020 research and innovation programme under Grant Agreement No 101008500 (PANACEA).
This work was supported by the Icelandic Research Fund, grant No. 239662, the University of Iceland Research Fund (S.Th.S) and a doctoral fellowship from the University of Iceland Research Fund (SC).

Simulations parameters and experimental conditions are available in the Supporting Information.

Notes and references

1 B. Reif, S. E. Ashbrook, L. Emsley and M. Hong, Solid-state NMR spectroscopy, *Nat Rev Methods Primers*, 2021, **1**, 1–23.
2 A. W. Overhauser, Polarization of Nuclei in Metals, *Phys. Rev.*, 1953, **92**, 411–415.
3 A. B. Barnes, G. De Paëpe, P. C. A. van der Wel, K.-N. Hu, C.-G. Joo, V. S. Bajaj, M. L. Mak-Jurkauskas, J. R. Sirigiri, J. Herzfeld, R. J. Temkin and R. G. Griffin, High-Field Dynamic Nuclear Polarization for Solid and Solution Biological NMR, *Appl Magn Reson*, 2008, **34**, 237–263.
4 M. Rosay, M. Blank and F. Engelke, Instrumentation for solid-state dynamic nuclear polarization with magic angle spinning NMR, *Journal of Magnetic Resonance*, 2016, **264**, 88–98.
5 T. Biedenbänder, V. Aladin, S. Saeidpour and B. Corzilius, Dynamic Nuclear Polarization for Sensitivity Enhancement in Biomolecular Solid-State NMR, *Chem. Rev.*, 2022, **122**, 9738–9794.
6 W. Y. Chow, G. De Paëpe and S. Hediger, Biomolecular and Biological Applications of Solid-State NMR with Dynamic Nuclear Polarization Enhancement, *Chem. Rev.*, 2022, **122**, 9795–9847.
7 N. Ghassemi, A. Poulhazan, F. Deligey, F. Mentink-Vigier, I. Marcotte and T. Wang, Solid-State NMR Investigations of Extracellular Matrixes and Cell Walls of Algae, Bacteria, Fungi, and Plants, *Chem. Rev.*, 2022, **122**, 10036–10086.
8 A. J. Rossini, A. Zagdoun, M. Lelli, A. Lesage, C. Copéret and L. Emsley, Dynamic Nuclear Polarization Surface Enhanced NMR Spectroscopy, *Acc. Chem. Res.*, 2013, **46**, 1942–1951.
9 A. G. M. Rankin, J. Trébosc, F. Pourpoint, J.-P. Amoureux and O. Lafon, Recent developments in MAS DNP-NMR of materials, *Solid State Nuclear Magnetic Resonance*, 2019, **101**, 116–143.
10 A. S. Lilly Thankamony, J. J. Wittmann, M. Kaushik and B. Corzilius, Dynamic nuclear polarization for sensitivity enhancement in modern solid-state NMR, *Progress in Nuclear Magnetic Resonance Spectroscopy*, 2017, **102–103**, 120–195.
11 A. Venkatesh, A. Lund, L. Rochlitz, R. Jabbour, C. P. Gordon, G. Menzildjian, J. Viger-Gravel, P. Berruyer, D. Gajan, C. Copéret, A. Lesage and A. J. Rossini, The Structure of Molecular and Surface Platinum Sites Determined by DNP-SENS and Fast MAS 195Pt Solid-State NMR Spectroscopy, *J. Am. Chem. Soc.*, 2020, **142**, 18936–18945.
12 W.-C. Liao, B. Ghaffari, C. P. Gordon, J. Xu and C. Copéret, Dynamic Nuclear Polarization Surface Enhanced NMR spectroscopy (DNP SENS): Principles, protocols, and practice, *Current Opinion in Colloid & Interface Science*, 2018, **33**, 63–71.
13 F. Deligey, M. A. Frank, S. H. Cho, A. Kirui, F. Mentink-Vigier, M. T. Swulius, B. T. Nixon and T. Wang, Structure of *In Vitro* -Synthesized Cellulose Fibrils Viewed by Cryo-Electron Tomography and ^{13}C Natural-Abundance Dynamic Nuclear Polarization Solid-State NMR, *Biomacromolecules*, 2022, **23**, 2290–2301.
14 O. Lafon, M. Rosay, F. Aussenac, X. Lu, J. Trébosc, O. Cristini, C. Kinowski, N. Touati, H. Vezin and J.-P. Amoureux, Beyond the Silica Surface by Direct Silicon-29 Dynamic Nuclear Polarization, *Angew. Chem. Int. Ed.*, 2011, **50**, 8367–8370.
15 A. Lesage, M. Lelli, D. Gajan, M. A. Caporini, V. Vitzthum, P. Miéville, J. Alauzun, A. Roussey, C. Thieuleux, A. Mehdi, G. Bodenhausen, C. Coperet and L. Emsley, Surface Enhanced NMR Spectroscopy by Dynamic Nuclear Polarization, *J. Am. Chem. Soc.*, 2010, **132**, 15459–15461.
16 D. Lee, N. T. Duong, O. Lafon and G. De Paëpe, Primostrato Solid-State NMR Enhanced by Dynamic Nuclear Polarization: Pentacoordinated Al $^{3+}$ Ions Are Only Located at the Surface of Hydrated γ-Alumina, *J. Phys. Chem. C*, 2014, **118**, 25065–25076.
17 A. J. Rossini, A. Zagdoun, M. Lelli, J. Canivet, S. Aguado, O. Ouari, P. Tordo, M. Rosay, W. E. Maas, C. Copéret, D. Farrusseng, L. Emsley and A. Lesage, Dynamic Nuclear Polarization Enhanced Solid-State NMR Spectroscopy of Functionalized Metal-Organic Frameworks, *Angew. Chem. Int. Ed.*, 2012, **51**, 123–127.
18 Y. Chen, R. W. Dorn, M. P. Hanrahan, L. Wei, R. Blome-Fernández, A. M. Medina-Gonzalez, M. A. S. Adamson, A. H. Flintgruber, J. Vela and A. J. Rossini, Revealing the Surface Structure of CdSe Nanocrystals by Dynamic Nuclear Polarization-Enhanced ^{77}Se and ^{113}Cd Solid-State NMR Spectroscopy, *J. Am. Chem. Soc.*, 2021, **143**, 8747–8760.
19 D. Lee, C. Leroy, C. Crevant, L. Bonhomme-Coury, F. Babonneau, D. Laurencin, C. Bonhomme and G. De Paëpe, Interfacial Ca2+ environments in nanocrystalline apatites revealed by dynamic nuclear polarization enhanced 43Ca NMR spectroscopy, *Nat Commun*, 2017, **8**, 14104.
20 W. Y. Chow, R. Li, I. Goldberga, D. G. Reid, R. Rajan, J. Clark, H. Oschkinat, M. J. Duer, R. Hayward and C. M. Shanahan, Essential but sparse collagen hydroxylysyl post-translational modifications detected by DNP NMR, *Chem. Commun.*, 2018, **54**, 12570–12573.
21 K. Jaudzems, T. Polenova, G. Pintacuda, H. Oschkinat and A. Lesage, DNP NMR of biomolecular assemblies, *Journal of Structural Biology*, 2019, **206**, 90–98.
22 K. K. Frederick, V. K. Michaelis, B. Corzilius, T.-C. Ong, A. C. Jacavone, R. G. Griffin and S. Lindquist, Sensitivity-Enhanced NMR Reveals Alterations in Protein Structure by Cellular Milieus, *Cell*, 2015, **163**, 620–628.
23 A. N. Smith, K. Märker, T. Piretra, J. C. Boatz, I. Matlahov, R. Kodali, S. Hediger, P. C. A. van der Wel and G. De Paëpe, Structural Fingerprinting of Protein Aggregates by Dynamic Nuclear Polarization-Enhanced Solid-State NMR at Natural Isotopic Abundance, *J. Am. Chem. Soc.*, 2018, **140**, 14576–14580.
24 F. A. Perras, T. Kobayashi and M. Pruski, Natural Abundance 17O DNP Two-Dimensional and Surface-Enhanced NMR Spectroscopy, *J. Am. Chem. Soc.*, 2015, **137**, 8336–8339.

25 K. Märker, S. Paul, C. Fernández-de-Alba, D. Lee, J.-M. Mouesca, S. Hediger and G. De Paëpe, Welcoming natural isotopic abundance in solid-state NMR: probing π-stacking and supramolecular structure of organic nanoassemblies using DNP, *Chem. Sci.*, 2017, **8**, 974–987.

26 H. Takahashi, D. Lee, L. Dubois, M. Bardet, S. Hediger and G. De Paëpe, Rapid Natural-Abundance 2D ^{13}C-^{13}C Correlation Spectroscopy Using Dynamic Nuclear Polarization Enhanced Solid-State NMR and Matrix-Free Sample Preparation, *Angew. Chem. Int. Ed.*, 2012, **51**, 11766–11769.

27 M. P. Hanrahan, Y. Chen, R. Blome-Fernández, J. L. Stein, G. F. Pach, M. A. S. Adamson, N. R. Neale, B. M. Cossairt, J. Vela and A. J. Rossini, Probing the Surface Structure of Semiconductor Nanoparticles by DNP SENS with Dielectric Support Materials, *J. Am. Chem. Soc.*, 2019, **141**, 15532–15546.

28 K.-N. Hu, H. Yu, T. M. Swager and R. G. Griffin, Dynamic Nuclear Polarization with Biradicals, *J. Am. Chem. Soc.*, 2004, **126**, 10844–10845.

29 G. Casano, H. Karoui and O. Ouari, Polarizing Agents: Evolution and Outlook in Free Radical Development for DNP, , DOI:10.1002/9780470034590.emrstm1547.

30 F. Mentink-Vigier, Ü. Akbey, Y. Hovav, S. Vega, H. Oschkinat and A. Feintuch, Fast passage dynamic nuclear polarization on rotating solids, *Journal of Magnetic Resonance*, 2012, **224**, 13–21.

31 K. R. Thurber and R. Tycko, Theory for cross effect dynamic nuclear polarization under magic-angle spinning in solid state nuclear magnetic resonance: The importance of level crossings, *The Journal of Chemical Physics*, 2012, **137**, 084508.

32 F. Mentink-Vigier, Ü. Akbey, H. Oschkinat, S. Vega and A. Feintuch, Theoretical aspects of Magic Angle Spinning - Dynamic Nuclear Polarization, *Journal of Magnetic Resonance*, 2015, **258**, 102–120.

33 S. Hediger, D. Lee, F. Mentink-Vigier and G. De Paëpe, in *eMagRes*, John Wiley & Sons, Ltd, 2018, pp. 105–116.

34 A. Pines, M. G. Gibby and J. S. Waugh, Proton-enhanced NMR of dilute spins in solids, *The Journal of Chemical Physics*, 1973, **59**, 569–590.

35 Y. Matsuki, T. Maly, O. Ouari, H. Karoui, F. Le Moigne, E. Rizzato, S. Lyubenova, J. Herzfeld, T. Prisner, P. Tordo and R. G. Griffin, Dynamic Nuclear Polarization with a Rigid Biradical, *Angew. Chem. Int. Ed.*, 2009, **48**, 4996–5000.

36 F. Mentink-Vigier, Optimizing nitroxide biradicals for cross-effect MAS-DNP: the role of *g* -tensors' distance, *Phys. Chem. Chem. Phys.*, 2020, **22**, 3643–3652.

37 F. A. Perras, A. Sadow and M. Pruski, In Silico Design of DNP Polarizing Agents: Can Current Dinitroxides Be Improved?, *ChemPhysChem*, 2017, **18**, 2279–2287.

38 C. Ysacco, H. Karoui, G. Casano, F. Le Moigne, S. Combes, A. Rockenbauer, M. Rosay, W. Maas, O. Ouari and P. Tordo, Dinitroxides for Solid State Dynamic Nuclear Polarization, *Appl Magn Reson*, 2012, **43**, 251–261.

39 C. Song, K.-N. Hu, C.-G. Joo, T. M. Swager and R. G. Griffin, TOTAPOL: A Biradical Polarizing Agent for Dynamic Nuclear Polarization Experiments in Aqueous Media, *J. Am. Chem. Soc.*, 2006, **128**, 11385–11390.

40 F. Mentink-Vigier, I. Marin-Montesinos, A. P. Jagtap, T. Halbritter, J. van Tol, S. Hediger, D. Lee, S. Th. Sigurdsson and G. De Paëpe, Computationally Assisted Design of Polarizing Agents for Dynamic Nuclear Polarization Enhanced NMR: The AsymPol Family, *J. Am. Chem. Soc.*, 2018, **140**, 11013–11019.

41 R. Harrabi, T. Halbritter, F. Aussenac, O. Dakhlaoui, J. van Tol, K. K. Damodaran, D. Lee, S. Paul, S. Hediger, F. Mentink-Vigier, S. Th. Sigurdsson and G. De Paëpe, Highly Efficient Polarizing Agents for MAS-DNP of Proton-Dense Molecular Solids, *Angewandte Chemie International Edition*, 2022, **61**, e202114103.

42 G. Mathies, M. A. Caporini, V. K. Michaelis, Y. Liu, K.-N. Hu, D. Mance, J. L. Zweier, M. Rosay, M. Baldus and R. G. Griffin, Efficient Dynamic Nuclear Polarization at 800 MHz/527 GHz with Trityl-Nitroxide Biradicals, *Angew. Chem.*, 2015, **127**, 11936–11940.

43 A. Equbal, K. Tagami and S. Han, Balancing dipolar and exchange coupling in biradicals to maximize cross effect dynamic nuclear polarization, *Phys. Chem. Chem. Phys.*, 2020, **22**, 13569–13579.

44 F. Mentink-Vigier, G. Mathies, Y. Liu, A.-L. Barra, M. A. Caporini, D. Lee, S. Hediger, R. G. Griffin and G. De Paëpe, Efficient cross-effect dynamic nuclear polarization without depolarization in high-resolution MAS NMR, *Chem. Sci.*, 2017, **8**, 8150–8163.

45 A. Zagdoun, G. Casano, O. Ouari, G. Lapadula, A. J. Rossini, M. Lelli, M. Baffert, D. Gajan, L. Veyre, W. E. Maas, M. Rosay, R. T. Weber, C. Thieuleux, C. Copéret, A. Lesage, P. Tordo and L. Emsley, A Slowly Relaxing Rigid Biradical for Efficient Dynamic Nuclear Polarization Surface-Enhanced NMR Spectroscopy: Expeditious Characterization of Functional Group Manipulation in Hybrid Materials, *J. Am. Chem. Soc.*, 2012, **134**, 2284–2291.

46 C. Sauvée, G. Casano, S. Abel, A. Rockenbauer, D. Akhmetzyanov, H. Karoui, D. Siri, F. Aussenac, W. Maas, R. T. Weber, T. Prisner, M. Rosay, P. Tordo and O. Ouari, Tailoring of Polarizing Agents in the bTurea Series for Cross-Effect Dynamic Nuclear Polarization in Aqueous Media, *Chem. Eur. J.*, 2016, **22**, 5598–5606.

47 D. J. Kubicki, G. Casano, M. Schwarzwälder, S. Abel, C. Sauvée, K. Ganesan, M. Yulikov, A. J. Rossini, G. Jeschke, C. Copéret, A. Lesage, P. Tordo, O. Ouari and L. Emsley, Rational design of dinitroxide biradicals for efficient cross-effect dynamic nuclear polarization, *Chem. Sci.*, 2016, **7**, 550–558.

48 A. P. Jagtap, M.-A. Geiger, D. Stöppler, M. Orwick-Rydmark, H. Oschkinat and S. Th. Sigurdsson, bcTol: a highly water-soluble biradical for efficient dynamic nuclear polarization of biomolecules, *Chem. Commun.*, 2016, **52**, 7020–7023.

49 M. A. Geiger, A. P. Jagtap, M. Kaushik, H. Sun, D. Stöppler, S. T. Sigurdsson, B. Corzilius and H. Oschkinat, Efficiency of Water-Soluble Nitroxide Biradicals for Dynamic Nuclear Polarization in Rotating Solids at 9.4 T: bcTol-M and cyolyl-TOTAPOL as New Polarizing Agents, *Chemistry - A European Journal*, 2018, **24**, 13485–13494.

50 A. Venkatesh, G. Casano, Y. Rao, F. De Biasi, F. A. Perras, D. J. Kubicki, D. Siri, S. Abel, H. Karoui, M. Yulikov, O. Ouari and L. Emsley, Deuterated TEKPol Biradicals and the Spin-Diffusion Barrier in MAS DNP, *Angew Chem Int Ed*, 2023, **62**, e202304844.

51 F. Mentink-Vigier, S. Paul, D. Lee, A. Feintuch, S. Hediger, S. Vega and G. De Paëpe, Nuclear depolarization and absolute sensitivity in magic-angle spinning cross effect dynamic nuclear polarization, *Phys. Chem. Chem. Phys.*, 2015, **17**, 21824–21836.

52 K. R. Thurber and R. Tycko, Perturbation of nuclear spin polarizations in solid state NMR of nitroxide-doped samples by magic-angle spinning without microwaves, *The Journal of Chemical Physics*, 2014, **140**, 184201.

53 F. Mentink-Vigier, S. Vega and G. De Paepe, Fast and accurate MAS–DNP simulations of large spin ensembles, *Physical Chemistry Chemical Physics*, 2017, **19**, 3506–3522.

54 M. Ernst and B. H. Meier, in *Studies in Physical and Theoretical Chemistry*, Elsevier, 1998, vol. 84, pp. 83–121.
55 P. C. A. van der Wel, K.-N. Hu, J. Lewandowski and R. G. Griffin, Dynamic Nuclear Polarization of Amyloidogenic Peptide Nanocrystals: GNNQQNY, a Core Segment of the Yeast Prion Protein Sup35p, *J. Am. Chem. Soc.*, 2006, **128**, 10840–10846.
56 A. J. Rossini, A. Zagdoun, F. Hegner, M. Schwarzwälder, D. Gajan, C. Copéret, A. Lesage and L. Emsley, Dynamic Nuclear Polarization NMR Spectroscopy of Microcrystalline Solids, *J. Am. Chem. Soc.*, 2012, **134**, 16899–16908.
57 N. A. Prisco, A. C. Pinon, L. Emsley and B. F. Chmelka, Scaling analyses for hyperpolarization transfer across a spin-diffusion barrier and into bulk solid media, *Phys. Chem. Chem. Phys.*, 2021, **23**, 1006–1020.
58 Q. Stern, S. F. Cousin, F. Mentink-Vigier, A. C. Pinon, S. J. Elliott, O. Cala and S. Jannin, Direct observation of hyperpolarization breaking through the spin diffusion barrier, *Science Advances*, 2021, **7**, eabf5735.
59 J. P. Wolfe, Direct Observation of a Nuclear Spin Diffusion Barrier, *Phys. Rev. Lett.*, 1973, **31**, 907–910.
60 A. A. Smith, B. Corzilius, A. B. Barnes, T. Maly and R. G. Griffin, Solid effect dynamic nuclear polarization and polarization pathways, *The Journal of Chemical Physics*, 2012, **136**, 015101.
61 F. Mentink-Vigier, A.-L. Barra, J. van Tol, S. Hediger, D. Lee and G. De Paepe, De novo prediction of cross-effect efficiency for magic angle spinning dynamic nuclear polarization, *Physical Chemistry Chemical Physics*, 2019, **21**, 2166–2176.
62 F. A. Perras, M. Raju, S. L. Carnahan, D. Akbarian, A. C. T. van Duin, A. J. Rossini and M. Pruski, Full-Scale Ab Initio Simulation of Magic-Angle-Spinning Dynamic Nuclear Polarization, *J. Phys. Chem. Lett.*, 2020, **11**, 5655–5660.
63 F. Mentink-Vigier, T. Dubroca, J. Van Tol and S. Th. Sigurdsson, The distance between g-tensors of nitroxide biradicals governs MAS-DNP performance: The case of the bTurea family, *Journal of Magnetic Resonance*, 2021, **329**, 107026.
64 F. A. Perras and M. Pruski, Large-scale *ab initio* simulations of MAS DNP enhancements using a Monte Carlo optimization strategy, *The Journal of Chemical Physics*, 2018, **149**, 154202.
65 M. Gafurov, S. Lyubenova, V. Denysenkov, O. Ouari, H. Karoui, F. Le Moigne, P. Tordo and T. Prisner, EPR Characterization of a Rigid Bis-TEMPO–Bis-Ketal for Dynamic Nuclear Polarization, *Appl Magn Reson*, 2010, **37**, 505–514.
66 A. Zagdoun, G. Casano, O. Ouari, M. Schwarzwälder, A. J. Rossini, F. Aussenac, M. Yulikov, G. Jeschke, C. Copéret, A. Lesage, P. Tordo and L. Emsley, Large Molecular Weight Nitroxide Biradicals Providing Efficient Dynamic Nuclear Polarization at Temperatures up to 200 K, *J. Am. Chem. Soc.*, 2013, **135**, 12790–12797.
67 C. Sauvée, M. Rosay, G. Casano, F. Aussenac, R. T. Weber, O. Ouari and P. Tordo, Highly Efficient, Water-Soluble Polarizing Agents for Dynamic Nuclear Polarization at High Frequency, *Angew. Chem. Int. Ed.*, 2013, **52**, 10858–10861.
68 A. Lund, G. Casano, G. Menzildjian, M. Kaushik, G. Stevanato, M. Yulikov, R. Jabbour, D. Wisser, M. Renom-Carrasco, C. Thieuleux, F. Bernada, H. Karoui, D. Siri, M. Rosay, I. V. Sergeyev, D. Gajan, M. Lelli, L. Emsley, O. Ouari and A. Lesage, TinyPols: a family of water-soluble binitroxides tailored for dynamic nuclear polarization enhanced NMR spectroscopy at 18.8 and 21.1 T, *Chem. Sci.*, 2020, **11**, 2810–2818.
69 S. R. Chaudhari, P. Berruyer, D. Gajan, C. Reiter, F. Engelke, D. L. Silverio, C. Copéret, M. Lelli, A. Lesage and L. Emsley, Dynamic nuclear polarization at 40 kHz magic angle spinning, *Phys. Chem. Chem. Phys.*, 2016, **18**, 10616–10622.
70 J. Soetbeer, P. Gast, J. J. Walish, Y. Zhao, C. George, C. Yang, T. M. Swager, R. G. Griffin and G. Mathies, Conformation of bis-nitroxide polarizing agents by multi-frequency EPR spectroscopy, *Phys. Chem. Chem. Phys.*, 2018, **20**, 25506–25517.
71 F. A. Perras, S. L. Carnahan, W.-S. Lo, C. J. Ward, J. Yu, W. Huang and A. J. Rossini, Hybrid quantum-classical simulations of magic angle spinning dynamic nuclear polarization in very large spin systems, *J. Chem. Phys.*, 2022, **156**, 124112.
72 F. A. Perras, R. R. Reinig, I. I. Slowing, A. D. Sadow and M. Pruski, Effects of biradical deuteration on the performance of DNP: towards better performing polarizing agents, *Phys. Chem. Chem. Phys.*, 2016, **18**, 65–69.
73 M. A. Geiger, M. Orwick-Rydmark, K. Märker, W. T. Franks, D. Akhmetzyanov, D. Stöppler, M. Zinke, E. Specker, M. Nazaré, A. Diehl, B.-J. van Rossum, F. Aussenac, T. F. Prisner, U. Akbey and H. Oschkinat, Temperature dependence of cross-effect dynamic nuclear polarization in rotating solids: advantages of elevated temperatures, *Phys. Chem. Chem. Phys.*, 2016, **18**, 30696–30704.
74 D. Wisser, G. Karthikeyan, A. Lund, G. Casano, H. Karoui, M. Yulikov, G. Menzildjian, A. C. Pinon, A. Purea, F. Engelke, S. R. Chaudhari, D. Kubicki, A. J. Rossini, I. B. Moroz, D. Gajan, C. Copéret, G. Jeschke, M. Lelli, L. Emsley, A. Lesage and O. Ouari, BDPA-Nitroxide Biradicals Tailored for Efficient Dynamic Nuclear Polarization Enhanced Solid-State NMR at Magnetic Fields up to 21.1 T, *J. Am. Chem. Soc.*, 2018, **140**, 13340–13349.
75 T. Halbritter, R. Harrabi, S. Paul, J. Van Tol, D. Lee, S. Hediger, S. Th. Sigurdsson, F. Mentink-Vigier and G. De Paëpe, PyrroTriPol: a semi-rigid trityl-nitroxide for high field dynamic nuclear polarization, *Chem. Sci.*, 2023, **14**, 3852–3864.